

Article

Kinetics of Heavy Reformate Conversion to Xylenes over MCM-41 on Zeolite Beta Composite Catalyst

Syed Ahmed Ali¹ and Mohammad Mozahar Hossain^{1,2,*} 

¹ Center for Refining and Advanced Chemicals, King Fahd University of Petroleum and Minerals, Dhahran 31261, Saudi Arabia

² Department of Chemical Engineering, King Fahd University of Petroleum and Minerals, Dhahran 31261, Saudi Arabia

* Correspondence: mhossain@kfupm.edu.sa; Tel.: +966-13-860-1478

Abstract: Commercial heavy reformate is converted over MCM-41 on zeolite beta composite catalyst to produce mixed xylenes in a fluidized-bed batch reactor. The heavy reformate feedstock contains 67.4 wt.% trimethyl benzenes (TMBs) and 31.1 wt.% methyl ethyl benzenes (MEBs). The experiments were carried out at 300, 350 and 400 °C, while the reaction times were varied between 5 and 20 s. The conversion of MEBs was more than two times the conversion of TMBs. The selectivity to xylenes was quite high (60–65 wt.%) but changed very little with reaction time or temperature. A kinetic model was developed using a five-reaction network. The product composition obtained from the estimated kinetic parameters closely matches the experimental results, which confirms the validity of the assumptions made for kinetic modeling. The trend in the apparent activation energies of the reactions was in accordance with the relative size of the reactant molecules, and the lowest activation energy was for the transalkylation of TMBs with toluene to produce xylenes.

Keywords: reformate; xylene; kinetic modelling; transalkylation; composite catalyst



Citation: Ali, S.A.; Hossain, M.M. Kinetics of Heavy Reformate Conversion to Xylenes over MCM-41 on Zeolite Beta Composite Catalyst. *Catalysts* **2023**, *13*, 335. <https://doi.org/10.3390/catal13020335>

Academic Editor: Joris W. Thybaut

Received: 5 January 2023

Revised: 23 January 2023

Accepted: 30 January 2023

Published: 2 February 2023



Copyright: © 2023 by the authors. Licensee MDPI, Basel, Switzerland. This article is an open access article distributed under the terms and conditions of the Creative Commons Attribution (CC BY) license (<https://creativecommons.org/licenses/by/4.0/>).

1. Introduction

Statutory decrees which limit the aromatics content in gasoline compel the refining and petrochemical industry to seek cost-effective alternatives for the utilization of heavy reformate. At the same time, the demand for xylenes is increasing due to the consumption of para-xylene in polyester manufacturing. The process which converts heavy reformate to xylenes consists of dealkylation, transalkylation, disproportionation, isomerization and other side reactions that occur sequentially and/or simultaneously [1]. Therefore, the process requires not only an active but also a selective and stable catalyst. Studies have shown that the catalytic process for heavy reformate conversion into xylenes is significantly affected by the topology and the type of zeolite as well as the strength of its acid sites [2–5]. Bifunctional catalysts, consisting of a mild hydrogenating metal on an acidic support, are reported to be suitable for xylene formation [1,6–9].

In addition to medium- and large-pore zeolites, hierarchical composite catalysts have been developed which possesses a suitable micro- and meso-porous structure. Such hierarchical composite catalysts can overcome some of the shortcomings of a conventional large-pore zeolite [10,11]. Ali et al. [12] reported improved performance of hierarchical composites of MCM-41 on zeolite beta synthesized by in-situ hydrothermal technique compared to the parent zeolite. MCM-41 is a well-ordered mesoporous material which has been reported as an excellent catalytic material [13,14].

While research has mostly focused on the development of various catalyst formulations that promote the transformation of C9 aromatics to xylenes, only a limited number of reports have been published on the reaction network and kinetic modeling. Waziri et al. [15] studied the kinetics of the transalkylation, disproportionation, and isomerization of model compounds (toluene and 1,2,4-trimethylbenzene) and their mixtures. Thakur et al. [16]

studied the transalkylation of 1,2,4-trimethylbenzene and toluene over cerium-modified zeolite catalyst. They applied the Langmuir–Hinshelwood–Hougen–Watson (LHHW) mechanism to estimate the kinetic parameters using nonlinear regression.

Kinetic modeling of methyl ethyl benzene (MEB) dealkylation, trimethylbenzene (TMB) disproportionation and its transalkylation with toluene was investigated by Ali et al. [17] over ZSM-5, mordenite and zeolite beta. The model compounds were mixed in appropriate ratios in order to prepare a simulated industrial feedstock. A four-reaction network was used for kinetic modeling. Al-Mubaiyedh et al. [18] reported a kinetic model for the conversion of heavy reformat over dual-zeolites (mordenite and ZSM-5) and reported the kinetic parameters. An elaborate reaction network and kinetic model was recently proposed by Khaksar et al. [19] for the disproportionation and transalkylation reactions of C9 and C10 aromatics on a commercial catalyst. They proposed a reaction network consisting of 12 reactions including transalkylation, disproportionation and hydrodealkylation. A detailed reaction network for the production of xylenes from heavy reformates using a differential evaluation technique was published by Hamedi et al. [20].

This paper reports the kinetic modeling of a conversion of heavy reformat into xylenes over a catalyst containing 4 wt.% Mo impregnated on a hierarchical composite of MCM-41 on zeolite beta. A reaction network consisting of five main reactions is proposed for the overall heavy reformat conversion process. A power-law model is applied for the kinetics of this reaction network, and the model fits the experimental data very well.

2. Results

2.1. Physicochemical Characterization of Catalyst

Table 1 presents the textural and acidic properties of parent zeolite β and synthesized catalyst. The BET surface area and total pore volume of the parent zeolite increased significantly through hierarchical pore generation. About 72% of the total porosity in the catalyst is in the mesoporous range, which facilitates the access of larger reactant molecules to catalyst active sites while maintaining crystallinity [19]. The total acidity of the catalyst, as determined by NH_3 -TPD, was 668 $\mu\text{mol/g}$. Therefore, the catalyst possesses sufficient mesoporous volume and acidity required for heavy reformat conversion to xylenes.

Table 1. Textural and acidic properties of catalyst.

Property	Parent Zeolite β	Catalyst
BET Surface Area (m^2/g)	567	714
Total Pore Volume (cm^3/g)	0.242	0.598
<i>t</i> -Plot Micropore Volume (cm^3/g)	0.182	0.167
Mesopore Volume (cm^3/g)	0.060	0.431
Average Pore Diameter (nm)	2.67	3.35
Total Acidity (NH_3 $\mu\text{mol/g}$)	768	668

2.2. Conversion of Heavy Reformat

The heavy reformat contains about 98.5 wt.% C9 aromatics comprised of 67.4 wt.% TMBs and 31.1 wt.% MEBs. Small amounts of C10 aromatics (0.6 wt.%) and xylenes (0.9 wt.%) were also present. The TMBs and MEBs present in the heavy reformat can undergo several reactions including dealkylation, transalkylation, disproportionation, isomerization and paring. Table 2 presents a list of key reactions that could occur under the reaction conditions in the presence of zeolitic catalyst [1]. Undesirable reactions, such as the formation of multi-ring aromatics, also occur, which leads to carbonaceous deposition (coke) inside the pores or on the outer surface of the crystallites [12,21].

Table 2. Key reactions during the conversion of heavy reformat to xylenes.

Reaction	Reactant(s)	Product(s)
Dealkylation	MEB	Toluene
	MEB	Xylene
Disproportionation	Toluene + Toluene	Benzene + Xylene
	MEB + MEB	Toluene + MDEB
	TMB + TMB	Xylene + TeMB
Transalkylation	Toluene + TMB	Xylene + Xylene
	Toluene + TMB	Benzene + TeMB
Paring	TeMB	Toluene + propylene

Abbreviations: TMB: trimethylbenzene(s); MEB: methylethylbenzene(s); DMEB: dimethylethylbenzene(s); TeMB: tetramethylbenzene(s).

In order to generate the catalyst performance data for kinetic modeling, the experiments were conducted by varying the reaction temperature (300, 350 and 400 °C) and reaction time (5.0, 7.5, 10.0, 12.5, 15.0, 17.5 and 20.0 s). Table 3 summarizes the feed and products composition as well as the conversion of C9 aromatics, MEBs and TMBs.

Table 3. Composition of feed and products obtained at various reaction temperatures and times.

Reaction Temperature (°C)	Reaction Time (s)	Feed/Product Composition (wt.%)					Conversion (wt.%)		
		MEBs	TMBs	Toluene	Xylenes	TeMBs	MEBs	TMBs	C9
Heavy Reformat Feed		31.08	67.35	0.00	0.91	0.65	-	-	-
300	5.0	22.58	59.38	2.57	11.11	4.35	27.34	11.83	16.73
	7.5	21.07	57.71	3.35	12.80	5.06	32.20	14.32	19.96
	10.0	19.54	56.01	4.14	14.52	5.79	37.13	16.83	23.24
	12.5	18.63	54.91	4.57	15.60	6.29	40.05	18.47	25.28
	15.0	17.72	53.80	5.01	16.69	6.78	42.99	20.12	27.34
	17.5	16.66	52.52	5.54	18.01	7.27	46.38	22.01	29.71
	20.0	15.63	51.35	6.08	19.17	7.77	49.72	23.76	31.95
350	5.0	20.58	57.53	4.40	13.54	3.95	33.77	14.58	20.64
	7.5	18.82	55.54	5.43	15.60	4.61	39.43	17.54	24.45
	10.0	17.03	53.51	6.49	17.69	5.28	45.21	20.54	28.33
	12.5	15.68	51.98	7.28	19.35	5.71	49.55	22.82	31.26
	15.0	14.32	50.43	8.08	21.03	6.14	53.93	25.12	34.22
	17.5	13.44	49.35	8.54	22.17	6.51	56.76	26.73	36.21
	20.0	12.51	48.09	9.51	23.03	6.86	59.75	28.60	38.43
400	5.0	19.75	56.34	6.08	14.67	3.15	36.44	16.34	22.69
	7.5	16.67	54.14	7.53	17.72	3.94	46.38	19.61	28.07
	10.0	14.34	51.83	9.02	20.07	4.74	53.85	23.04	32.77
	12.5	12.53	50.68	10.10	21.85	4.83	59.67	24.75	35.77
	15.0	11.23	49.00	11.10	23.78	4.88	63.87	27.24	38.80
	17.5	9.52	47.73	12.01	25.68	5.06	69.38	29.13	41.84
	20.0	8.28	45.45	13.78	27.36	5.13	73.36	32.52	45.41

The conversion of C9 aromatics increased with reaction temperature as well as reaction time. Figure 1 depicts the conversion of MEBs and TMBs and the yield of xylenes as a function of the reaction time and temperature. The conversion of MEBs was more than two times the conversion of TMBs under the process conditions. MEBs are more reactive, and their dealkylation reactions are kinetically controlled and not limited by thermodynamics. As a result, their conversion increased significantly with reaction time and temperature. In contrast, the effect of reaction time and temperature on TMBs conversion was modest. This could be due to thermodynamic limitation, which controls the composition of alkylaromatics mixture [17]. The calculated equilibrium alkylbenzenes composition under the reaction

conditions is as follows: benzene (3.17 wt.%), toluene (16.70 wt.%), xylenes (37.75 wt.%) TMBs (31.84 wt.%) and TeMBs (13.59 wt.%). Therefore, the maximum conversion of TMBs for the present heavy reformate feed can be only about 52 wt.%. Since the maximum conversion of TMBs observed in the present study is 32.5 wt.%, the reaction is in the kinetic regime. Moreover, the transalkylation reaction involves the combination of two reactants, which makes it slower than monomolecular reactions, such as the dealkylation of MEBs. The xylene yields increased modestly from about 19.1 wt.% at 300 °C to 27.4 wt.% at 400 °C after 20 s.

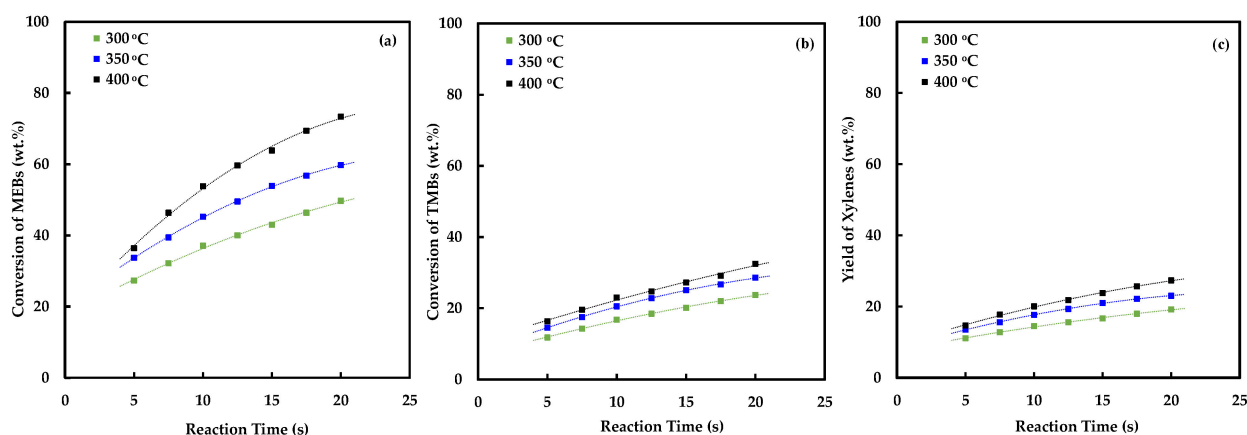


Figure 1. Conversion of MEBs (a), TMBs (b) and the yield of xylenes (c) as a function of reaction time and temperature.

The changes in the selectivity to xylenes, toluene and TeMBs versus reaction time and temperature is presented in Figure 2. The selectivity to xylenes is quite high (60–65 wt.%), but it changed very little with reaction time or temperature. Although the conversion of C9 aromatics as well as the yield of xylenes increased with reaction time and temperature, as shown in Table 1, the selectivity of xylenes remained almost unchanged. In contrast, the selectivity of toluene increased with both the reaction time and temperature. It increased from about 19 wt.% at 300 °C to 30.3 wt.% at 400 °C after 20 s. It should be noted that toluene is simultaneously produced by the dealkylation of MEBs and consumed in the transalkylation reaction. Similarly, the TeMBs are also produced by the disproportionation of TMBs and consumed in the paring reaction. The selectivity of TeMBs, however, decreased with reaction temperature, because the dependency of the rate of paring reaction on temperature is higher.

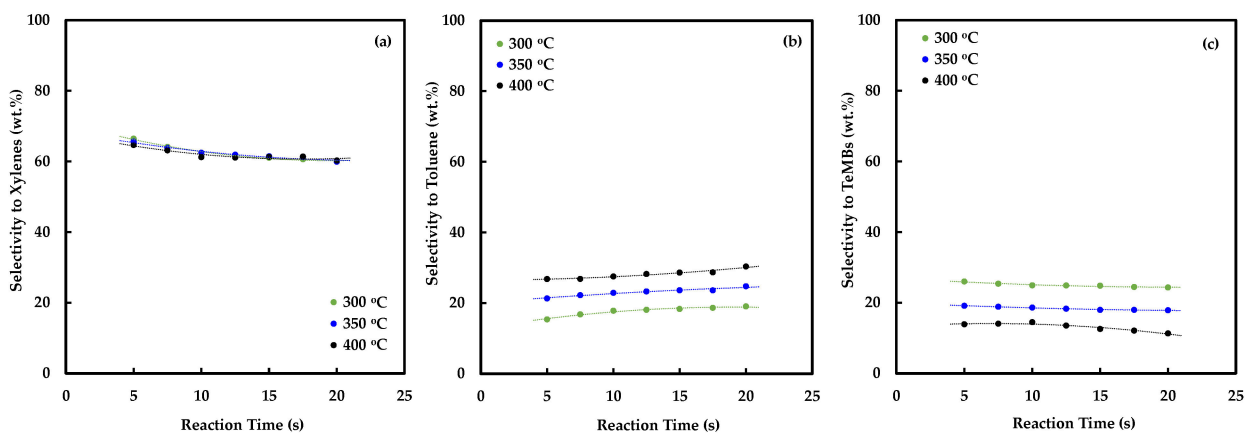


Figure 2. Selectivity towards xylenes (a), toluene (b) and TeMBs (c) as a function of reaction time and temperature.

It should be noted that the isomerization of xylenes, TMBs and MEBs also takes place during heavy reformate conversion. However, isomerization reactions are not included in the kinetic model, and the three isomers of xylenes are grouped together and considered as a single component. A similar approach was adopted for the isomers of TMBs and MEBs. Product composition shows the formation of negligible amounts of benzene and C1–C4 gases. The thermodynamic investigation also shows the formation of a low amount of benzene when the TMB/toluene ratio is about 2.5 (as is the case in this study) [18], hence the reactions that form benzene are not included in the kinetic model.

2.3. Model Formulation

On the basis of the product composition and of the results from other studies on transalkylation conducted by the authors' research group, a five-reaction network is proposed for kinetic modeling (Figure 3). The reactions considered are as follows:

- (i) dealkylation of MEBs to form toluene;
- (ii) disproportionation of TMBs to form TeMBs and xylenes;
- (iii) transalkylation of toluene and TMBs to form xylenes;
- (iv) paring reaction of TeMBs to form toluene; and
- (v) dealkylation of MEBs to form xylenes.

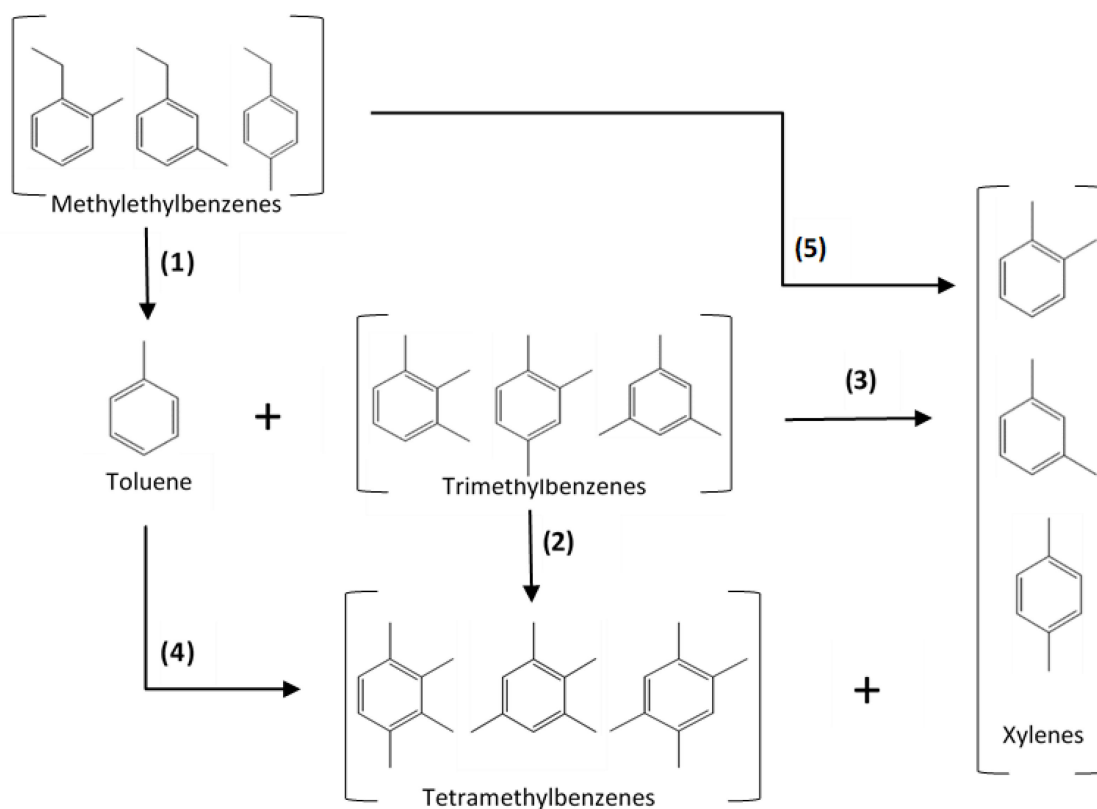


Figure 3. Simplified reaction network for kinetic modeling. Reactions (1) dealkylation of MEBs to form toluene; (2) disproportionation of TMBs to form TeMBs and xylenes; (3) transalkylation of toluene and TMBs to form xylenes; (4) paring reaction of TeMBs to form toluene; and (5) dealkylation of MEBs to form xylenes.

In order to further simplify the kinetic model, some additional assumptions were made, such as:

- (a) The five reactions are elementary;
- (b) The catalyst deactivation is defined by a single function for all of the reactions taking place; and

- (c) The reaction was conducted under isothermal conditions due to the fluidization of the reactants and catalyst particles.

The intrinsic rates of the discrete reaction steps can be correlated via an overall mole balance for the species involved during the conversion of heavy reformate. The following assumptions were made while formulating the mole balance equations:

- (a) The kinetic model presumes the occurrence of only catalytic reactions, and thermal conversion is not taken into consideration.
 (b) Considering the short reaction time (maximum 20 s) and low C9 aromatics conversions, the change in temperature during each run is negligible.
 (c) At any given instant, the concentrations of chemical species are effectively uniform due to the high intensity of gas recirculation and a short reaction time.
 (d) The concentration of coke is uniform due to the high degree of fluidization at any given time.

Rate of disappearance of MEBs

$$\frac{V}{W_c} \frac{dC_{MEBs}}{dt} = -(k_1 + k_5)C_{MEBs}\varphi \quad (1)$$

Rate of disproportionation of TMBs

$$\frac{V}{W_c} \frac{dC_{TMBs}}{dt} = -(2k_2C_{TMBs}^2 - k_3C_{TMBs}C_{toluene})\varphi \quad (2)$$

Rate of formation of toluene

$$\frac{V}{W_c} \frac{dC_{toluene}}{dt} = (k_1C_{MEBs} + k_4C_{TeMBs} - k_3C_{TMBs}C_{toluene})\varphi \quad (3)$$

Rate of formation of xylenes

$$\frac{V}{W_c} \frac{dC_{xylenes}}{dt} = (k_2C_{TMBs}^2 + k_3C_{TMBs}C_{toluene} + k_5C_{MEBs})\varphi \quad (4)$$

Rate of formation of TeMBs

$$\frac{V}{W_c} \frac{dC_{TeMBs}}{dt} = (k_2C_{TMBs}^2 - k_4C_{TeMBs}C_{toluene})\varphi \quad (5)$$

where C_i is the molar concentration of species i , V is the volume of the reactor, W_c is catalyst mass, t is the reaction time and φ is the catalyst decay function, which represents the loss of catalytic activity due to coke formation. The catalyst deactivation function φ for the reactant conversion model is defined as (Ali et al. 2012):

$$\varphi = \exp(-\lambda x) \quad (6)$$

where λ is catalyst deactivation constant and x is the conversion of C9 aromatics.

The molar concentration C_i of each species can be denoted in terms of its mass fraction y_i , which is a measurable quantity by gas chromatography, by the following correlation:

$$C_i = \frac{y_i W_{hc}}{MW_i V} \quad (7)$$

where W_{hc} is the weight of feedstock injected into the reactor, MW_i is the molecular weight of the species i and V is the volume of the reactor.

According to the Arrhenius equation, the reaction rate constant k_i for each of the reaction steps is a function of temperature and can be expressed as follows:

$$k_i = k_{i0} \exp \left[-\frac{E_i}{R} \left(\frac{1}{T} - \frac{1}{T_0} \right) \right] \quad (8)$$

where k_{i0} is the pre-exponential factor and E_i is the energy of activation of the reaction i .

2.4. Estimation of Kinetic Parameters and Model Evaluation

The kinetic parameters, incorporating the individual rate expressions and the catalyst deactivation expression, were evaluated by a least-squares fitting of the experimental data using MATLAB[®] software. The regression analysis was carried out by the Levenberg–Marquardt algorithm, while the differential equations were numerically solved by making use of the Runge–Kutta–Gill method. A total of 105 data points obtained from the experiments were used for the regression analysis, while the number of parameters to be estimated was 11. Therefore, the degree of freedom for the parameter estimation was more than 94 (degree of freedom = 105 – 11). This showed that a large amount experimental data was used to estimate the kinetic parameters. The following principles were also included in the estimation of the kinetic parameters:

- (i) The specific reaction rate and activation energy for each reaction should agree with the physical–chemical principles.
- (ii) The regression coefficient (R^2) should be close to unity.
- (iii) The sum of squares of the residuals (SSR) should be lower than an acceptable minimum value.
- (iv) The kinetic parameters should display low confidence interval spans.

3. Discussion

Table 4 presents the estimated values of the kinetics parameters and their corresponding 95% confidence limits. The k_0 values for monomolecular reactions were higher than the values for bimolecular reactions. The formation of toluene from MEBs (Reaction 1) requires higher activation energy than the formation of xylenes from MEBs (Reaction 5). The lowest activation energy is required for the transalkylation of TMB with toluene (11.46 kJ/mol), which compares well with the reported value of 11.2 kJ/mol for zeolite β [17]. Disproportionation of TMBs requires a somewhat higher activation energy of 16.8 kJ/mol, which is attributed to involvement of two large molecules in this reaction. However, the value of activation energy obtained in this study was much lower than the reported value 29.9 kJ/mol for zeolite β . This difference can be attributed to the difference between the porosity of parent zeolite β and the hierarchical catalyst, which has enhanced mesoporosity that allows for easier access to the reactants. Hence, lower activation energy is needed for TMBs' disproportionation. The highest apparent activation energy (46.3 kJ/mol) was observed for the paring reactions of TeMBs, which are the molecules with largest diameter. Other studies [17,20] also reported the highest apparent activation energy for the paring reaction of TeMBs among the heavy reformat conversion reactions. The catalyst deactivation, estimated as $\lambda = 0.41$, indicates very low coke formation.

Table 4. Estimated Kinetic Parameters.

Frequency Factors *		Activation Energy (kJ/mol)	
$k_{1,0}$	1.31 ± 0.06	E_1	29.25 ± 2.43
$k_{2,0}$	0.03 ± 0.00	E_2	16.82 ± 1.56
$k_{3,0}$	0.06 ± 0.01	E_3	11.46 ± 9.14
$k_{4,0}$	2.71 ± 0.15	E_4	46.33 ± 3.83
$k_{5,0}$	0.98 ± 0.04	E_5	19.54 ± 2.41
λ (deactivation) = 0.41 ± 0.15			

* k_i : units vary.

Figure 4 compares the experimentally obtained composition of products obtained at various reaction times and temperatures with those predicted by the kinetic model. The plots shown in this figure confirm that the model prediction is very close to the experimental values. The parity plots of the reactants and products presented in Figure 5 further confirm the accuracy of the kinetic model. The correlation coefficients for MEBs, TMBs, toluene, xylenes and TeMBs were 0.9892, 0.9906, 0.9926, 0.9877 and 0.9242, respectively. The lower value of the correlation coefficient for TeMBs can be attributed to the possibility of other reactions involving TeMBs. Moreover, the relative amounts of TeMBs in the product are much lower than other products, which could amplify the error in estimation.

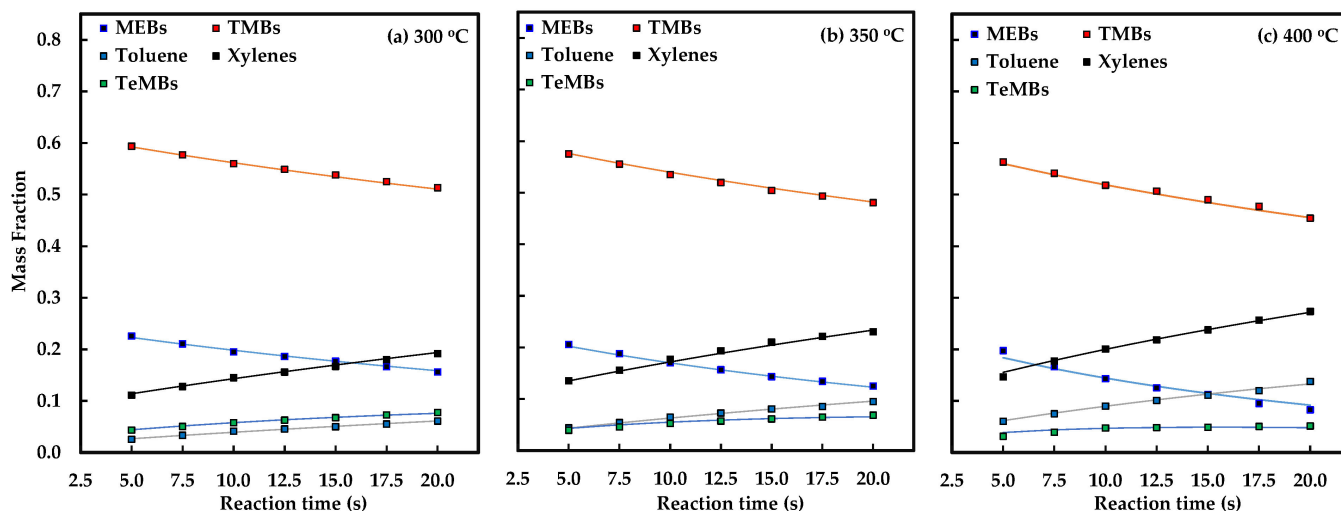


Figure 4. Products' composition versus reaction time at different temperatures. [Experimental data (symbols) and model predicted values (solid lines)].

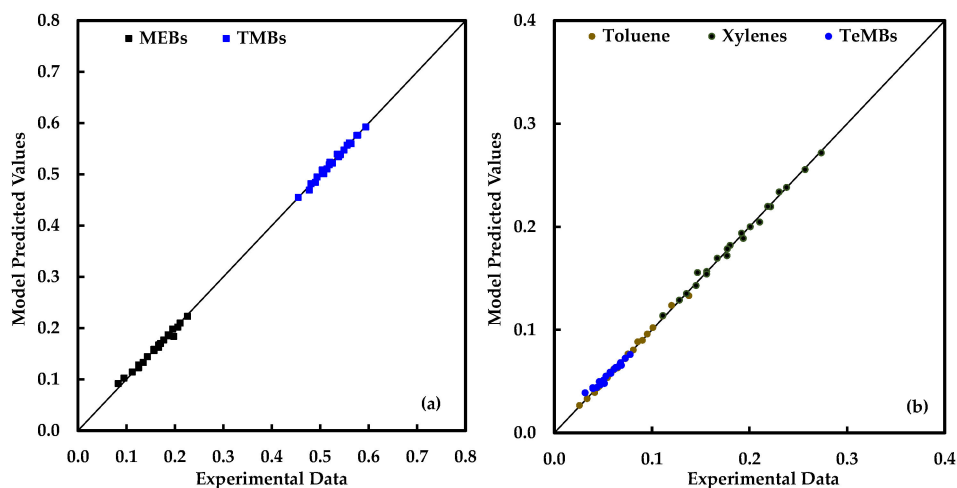


Figure 5. Parity plots showing the mass fractions of reactants (a) and products (b).

The reliability of the estimated kinetic parameters was confirmed by the negative slopes of the Arrhenius plots for the individual reaction rate constants, as presented in Figure 6 (for k_1 , k_2 , k_3 , k_4 and k_5). The error bars in this figure represent the range of $-\ln k$ values calculated from the 95% confidence limits of activation energies.

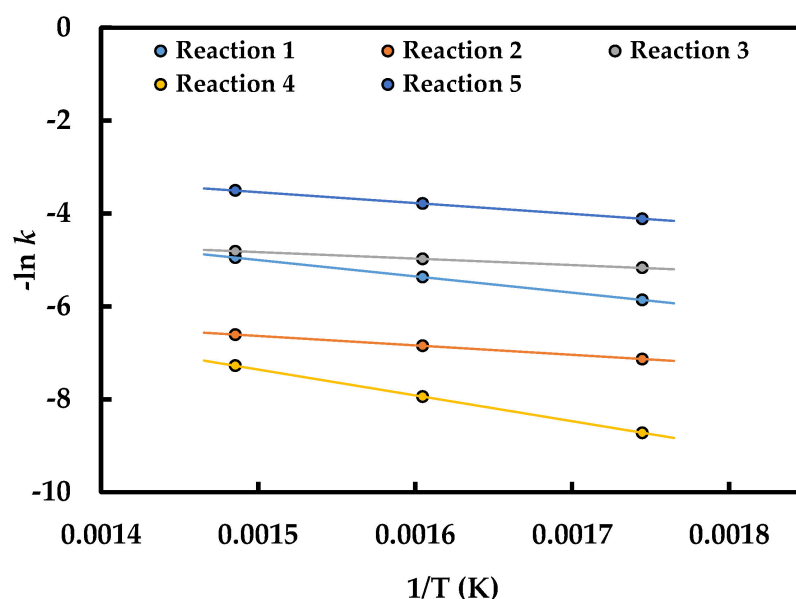


Figure 6. Arrhenius plots for the different reactions.

A comparison of the rates of different reactions is shown in Figure 7. A comparison between Reactions 2 and 3 shows that the rate of TMB-toluene transalkylation reaction is much higher than the TMB disproportionation. This is consistent with the earlier report, which found that the transalkylation of TMB is favored in the presence of toluene, while disproportionation is favored in the absence of toluene [2]. Paring reaction of TeMB is the slowest owing to the involvement of large molecules. It can be noted that the rate of MEB conversion by Reaction 5 (formation of xylenes) is much higher than Reaction 1 (formation of toluene). The conversion of MEBs over different zeolites was reported in our earlier paper [17]. From that MEB conversion study, it was concluded that the catalytic behavior of zeolites depends on their topology. When MEBs are reacted over zeolite β , higher amounts of xylenes are formed compared to mordenite and ZSM-5. The present study confirms that hierarchical catalyst also favors the direct formation of xylenes from MEBs (Reaction 5).

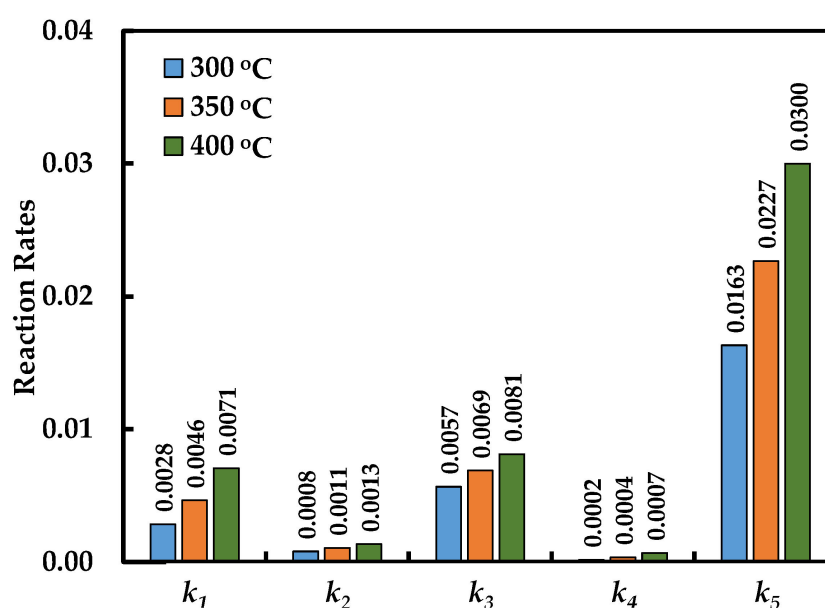


Figure 7. Comparison of rate constants of different reactions.

4. Materials and Methods

4.1. Materials

Parent zeolite beta ($\text{SiO}_2/\text{Al}_2\text{O}_3$ molar ratio = 38) was obtained from Tosoh Chemical Corporation, Japan for the preparation of catalyst. Ammonium heptamolybdate tetrahydrate $[(\text{NH}_4)_6\text{Mo}_7\text{O}_{24}\cdot 4\text{H}_2\text{O}]$ (> 99.3%) was employed as the source of molybdenum. Cetyl trimethyl ammonium bromide (CTAB) surfactant (> 98%) was used as an alkaline surfactant to dissolve the zeolites. These chemicals were procured from Sigma-Aldrich (St. Louis, MO, USA). Cataloid AP-3 alumina binder was obtained from Catalysts & Chemicals Industries Co., Ltd. (Yokohama, Japan) for the preparation of catalyst extrudates.

4.2. Catalyst Synthesis

The synthesis of hierarchical composite catalysts of MCM-41 on zeolite beta was carried out by an in situ hydrothermal technique. The hierarchical pore generation was achieved by 0.20 M NaOH solution during the disintegration of β -zeolite. The composite thus obtained was mixed with alumina binder and formed into a cylindrical shape by extrusion. The bifunctional catalyst was prepared by loading the composite zeolite with 4 wt.% molybdenum via an incipient wet impregnation method. The catalyst preparation procedure is described elsewhere [12].

4.3. Catalyst Characterization

The surface area and pore volume of the parent zeolite and synthesized catalyst was determined by nitrogen adsorption at $-196\text{ }^\circ\text{C}$ using a Micromeritics model ASAP 2020 analyzer. The sample was degassed by heating it under vacuum at a ramp rate of $10\text{ }^\circ\text{C}/\text{min}$ up to $350\text{ }^\circ\text{C}$ for six hours in order to remove moisture completely before the surface area (by BET method) and pore volume (by BJH method) measurements.

The NH_3 -TPD analysis was carried out in order to measure the acidity of the parent zeolite and the synthesized catalyst. A 100 mg sample was pretreated at $500\text{ }^\circ\text{C}$ for one hour in helium flowing at $50\text{ mL}/\text{min}$. After the sample had cooled down to room temperature, a mixture of 5 vol.% NH_3 and 95 vol.% He was introduced into the sample tube at $100\text{ }^\circ\text{C}$ for 0.5 h to saturate acid sites of the catalyst. The catalyst sample was heated at $120\text{ }^\circ\text{C}$ for two hours under helium flowing at $50\text{ mL}/\text{min}$ in order to remove the physisorbed ammonia. The desorption was conducted with a heating rate of $10\text{ }^\circ\text{C}/\text{min}$, and the emanating gas was detected using a thermal conductivity detector.

4.4. Generation of Catalyst Performance Data

Experiments to generate catalyst performance data for kinetic modeling were conducted in a CREC Riser Simulator, which is a fluidized batch reactor [22]. Figure 8 shows the schematic of the components of the riser simulator including the body of the reactor unit, impeller, and catalyst basket. The complete experimental setup is presented in Figure 9 [23]. This fluidized reactor system facilitates very short reaction times (5–20 s) and the accurate control of reaction conditions. The internal and external mass transfer restrictions were eliminated due to the very small size of catalyst particles (15–110 μm) and intense mixing, respectively. The volume of the reactor is 50 cm^3 , and the volume of the vacuum box is 1000 cm^3 .

The operation of the CREC Riser Simulator includes some preparatory steps prior to the initiation of the actual run with the catalyst loaded in the basket. These include (a) combusting any coke-on-catalyst with air; (b) heating the reactor to the reaction temperature, heating the vacuum box and the transporting lines to $250\text{ }^\circ\text{C}$; (c) conditioning the catalyst by contacting it with inert gas in order to remove the adsorbed species from a previous run; (d) evacuating the contents of the vacuum box, the 6 PV sample loop and the various lines in order to set them to a desirable low vacuum pressure (~ 4 psi); and (e) rotating the impeller at the preset rpm in order to achieve good fluidization.

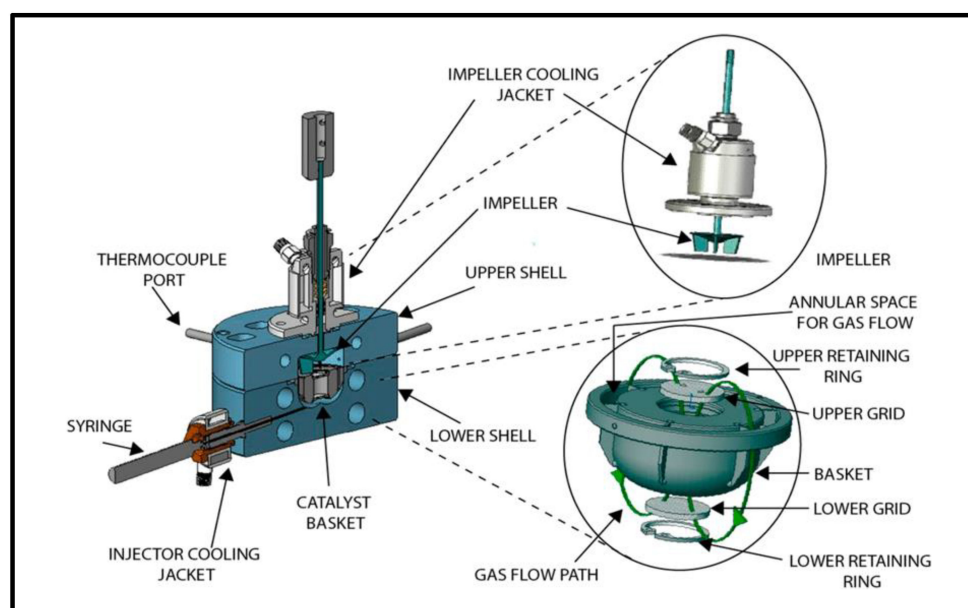


Figure 8. Schematic of the various components (body of the reactor unit, impeller and catalyst basket) of the CREC Riser Simulator [22,23].

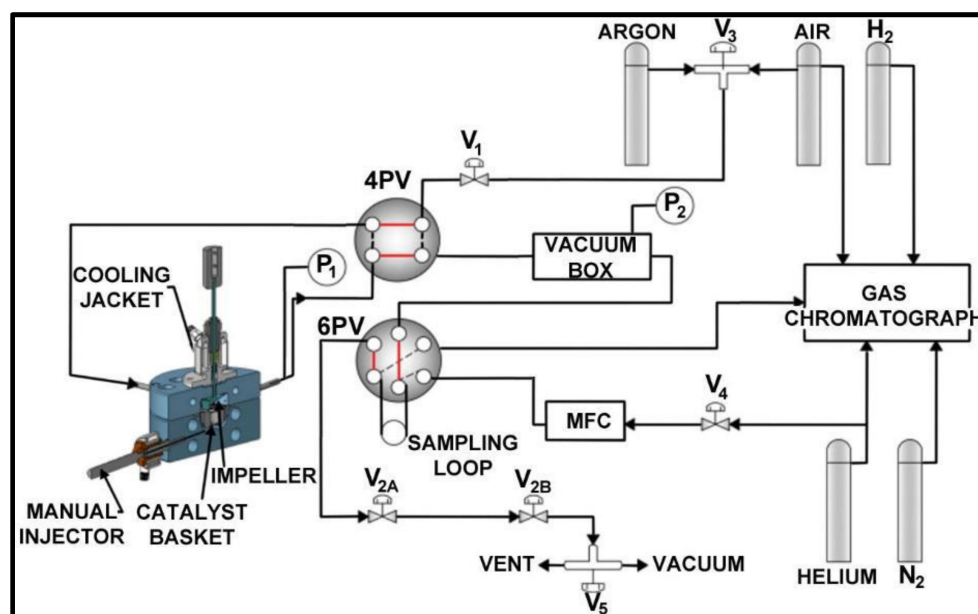


Figure 9. Schematic diagram of the CREC Riser Simulator experimental setup [22,23].

The transalkylation kinetics experiments were conducted at 300, 350 and 400 °C at a catalyst-to-reactant ratio of five for 5–20 s. During a typical test, 0.81 g of catalyst sample was loaded into the reactor basket and the system was purged with argon after ensuring the absence of leaks. The heating was started at a controlled rate to reach the target temperature. The flow of argon was maintained to keep the reaction atmosphere free from oxygen or hydrogen. When the desired reactor temperature was reached, the flow of argon was discontinued. The reactor isolation valve was closed when the desired pressure was reached, and the vacuum box was evacuated to 20.7 kPa.

The catalyst was fluidized by rotating the impeller, and 0.162 g of feed was injected into the reactor. The reaction was carried out for a specified time, and it was terminated by automatically opening the isolation valve between the reactor and the vacuum box. The unconverted reactants and products were moved into the vacuum box. The product

samples were analyzed using an Agilent 7890A GC fitted with TCD and FID detectors. The product composition was used to calculate the conversion of MEBs, TMBs and C9 aromatics and the selectivity of different species using the following equations:

$$\text{Conversion of MEBs (mass \%)} = \frac{\text{Mass of MEBs converted}}{\text{Mass of MEBs fed}} \times 100 \quad (9)$$

$$\text{Selectivity to species } i \text{ (mass \%)} = \frac{\text{Mass of product } i}{\text{Mass of C9 aromatics converted}} \times 100 \quad (10)$$

The catalyst was regenerated between every two runs in order to minimize the catalyst deactivation during the test. The reproducibility of the catalyst testing was confirmed by repeating some experiments, and the variation in product composition was within a range of $\pm 2\%$.

5. Conclusions

The kinetic modeling of heavy reformat conversion into xylenes over a hierarchical MCM-41 on zeolite β catalyst was carried out. The metal-loaded bifunctional composite catalyst with higher mesoporous volume than the parent zeolite facilitated better access to the large reactant molecules. The application of CREC Riser Simulator allowed for very short contact-time experiments with low-to-medium conversion suitable for kinetic modeling. Five key reactions including dealkylation, transalkylation, disproportionation and paring were selected to form a representative network for the kinetic modeling. The product composition obtained from the estimated kinetic parameters closely matches the experimental results at different temperatures and reaction times with an overall correlation coefficient of 0.9997. Thus, the results confirm the validity of the assumptions made for kinetic modeling. The five series-parallel reactions represent the experimental data quite accurately. Kinetic modeling results also show that the transalkylation reaction was significantly faster than the disproportionation reaction, indicating that the transfer of the methyl group from TMB to toluene is a preferred route under the reaction conditions studied. The high rate of the formation of xylenes directly from MEBs (Reaction 5) compared to the indirect route (Reaction 1) corroborates the earlier finding that the topology of catalyst plays a major role in the conversion of heavy reformat.

Author Contributions: Conceptualization, S.A.A. and M.M.H.; methodology, S.A.A. and M.M.H.; experimental work, S.A.A.; kinetic model development, M.M.H.; data curation, S.A.A.; writing—original draft preparation, S.A.A. and M.M.H.; reviewing and editing, S.A.A. and M.M.H. All authors have read and agreed to the published version of the manuscript.

Funding: This research received no external funding.

Data Availability Statement: The data presented in this study are available in this paper.

Acknowledgments: The author(s) would like to acknowledge the support provided by the Center for Refining and Advanced Chemicals and the Deanship of Research Oversight and Coordination at King Fahd University of Petroleum and Minerals (KFUPM) for funding this work through project No. DF191028.

Conflicts of Interest: The authors declare no conflict of interest.

References

1. Ali, S.A.; Al-Nawad, K.; Ercan, C.; Wang, Y. Parametric study of dealkylation-transalkylation reactions over mordenite-based bi-functional catalysts. *App. Catal. A Gen.* **2010**, *393*, 96–108. [[CrossRef](#)]
2. Wang, I.; Tsai, T.C.; Huang, S.T. Disproportionation of toluene and of trimethylbenzene and their transalkylation over zeolite beta. *Ind. Eng. Chem. Res.* **1990**, *29*, 2005–2012. [[CrossRef](#)]
3. Li, Y.; Wang, H.; Dong, M.; Li, J.; Qin, Z.; Wang, J.; Fan, W. Effect of zeolite pore structure on the diffusion and catalytic behaviors in the transalkylation of toluene with 1,2,4-trimethylbenzene. *RSC Adv.* **2015**, *5*, 66301–66310. [[CrossRef](#)]
4. Cha, S.; Hong, S. 1,2,4-Trimethylbenzene disproportionation over large-pore zeolites: An experimental and theoretical study. *J. Catal.* **2018**, *357*, 145–157. [[CrossRef](#)]

5. Almulla, F.M.; Ali, S.A.; Aldossary, M.R.; Alnaimi, E.I.; Jumah, A.B.; Garforth, A. Transalkylation of 1, 2, 4-trimethylbenzene with toluene over large pore zeolites: Role of pore structure and acidity. *Appl. Catal. A Gen.* **2020**, *608*, 117886. [[CrossRef](#)]
6. Krejci, A.; Al-Khattaf, S.; Ali, M.A.; Bejblova, M. Cejka, Transalkylation of toluene with trimethylbenzenes over large-pore zeolite. *Appl. Catal. A Gen.* **2010**, *377*, 99–106. [[CrossRef](#)]
7. Serra, J.; Guillon, E.; Corma, A. Optimizing the conversion of heavy reformat streams into xylenes with zeolite catalysts by using knowledge base high-throughput experimentation techniques. *J. Catal.* **2005**, *232*, 342–354. [[CrossRef](#)]
8. Tsai, T.C.; Liu, S.; Wang, I. Supported zeolite for heavy aromatics transalkylation process. *Catal. Surv. Asia* **2009**, *13*, 94–103. [[CrossRef](#)]
9. Al-Khattaf, S.; Ali, S.A.; Aitani, A.; Al-Nawad, K.; Chiu, C.; Tsai, T. Catalysis of metal supported zeolites for dealkylation-transalkylation of alkyl-aromatics. *Appl. Catal. A Gen.* **2016**, *514*, 154–163. [[CrossRef](#)]
10. Altindas, C.; Sher, F.; Smjecanin, N.; Lima, E.; Rashid, T.; Hai, I.; Karaduman, A. Synergistic interaction of metal loaded multifactorial nanocatalysts over bifunctional transalkylation for environmental applications. *Environ. Res.* **2023**, *216*, 114479. [[CrossRef](#)]
11. Margarit, V.J.; Portilla, M.T.; Navarro, M.T.; Abudawoud, R.; Al-Zahrani, I.M.; Shaikh, S.; Martínez, C.; Corma, A. One-pot co-crystallization of beta and pentasil nanozeolites for the direct conversion of a heavy reformat fraction into xylenes. *Appl. Catal. A Gen.* **2019**, *581*, 11–22. [[CrossRef](#)]
12. Ali, S.A.; Almulla, F.M.; Jermy, B.R.; Aitani, A.M.; Abudawoud, R.H.; AlAmer, M.A.; Qureshi, Z.S.; Mohammad, T.; Alasiri, H.S. Hierarchical composite catalysts of MCM-41 on zeolite beta for conversion of heavy reformat to xylenes. *J. Ind. Eng. Chem.* **2021**, *98*, 189–199. [[CrossRef](#)]
13. Salama, R.S.; El-Bahy, S.M.; Mannaa, M.A. Sulfamic acid supported on mesoporous MCM-41 as a novel, efficient and reusable heterogenous solid acid catalyst for synthesis of xanthene, dihydropyrimidinone and coumarin derivatives. *Colloids Surf. A Physicochem. Eng. Asp.* **2021**, *628*, 127261. [[CrossRef](#)]
14. El-Hakam, S.A.; Samra, S.E.; El-Dafrawy, S.M.; Ibrahim, A.A.; Salama, R.S. Surface acidity and catalytic activity of sulfated titania supported on mesoporous MCM-41. *Int. J. Mod. Chem.* **2013**, *5*, 55–70.
15. Waziri, S.; Aitani, A.M.; Al-Khattaf, S. Transformation of toluene and 1,2,4-trimethylbenzene over ZSM-5 and mordenite catalysts: A comprehensive kinetic model with reversibility. *Ind. Eng. Chem. Res.* **2010**, *49*, 6376–6387. [[CrossRef](#)]
16. Thakur, R.; Barman, S.; Gupta, R.K. Kinetic investigation in transalkylation of 1,2,4 trimethylbenzene with toluene over rare earth metal-modified large pore zeolite. *Chem. Eng. Commun.* **2017**, *204*, 254–264. [[CrossRef](#)]
17. Ali, S.A.; Ogunronbi, K.; Al-Khattaf, S. Kinetics of dealkylation-transalkylation of c9 alkyl-aromatics over zeolites of different structures. *Chem. Eng. Res. Des.* **2013**, *91*, 2601–2616. [[CrossRef](#)]
18. Al-Mubaiyedh, U.; Ali, S.A.; Al-Khattaf, S. Kinetic modeling of heavy reformat conversion into xylenes over mordenite-ZSM-5 based catalysts. *Chem. Eng. Res. Des.* **2012**, *90*, 1943–1955. [[CrossRef](#)]
19. Khaksar, S.A.N.; Farsi, M.; Khaksar, S.A. Kinetic modeling of gas-phase disproportionation and transalkylation of C9 and C10 aromatics over industrial zeolite catalyst. *React. Kin. Mech. Catal* **2021**, *32*, 1075–1093. [[CrossRef](#)]
20. Hamedi, N.; Iranshahi, D.; Rahimpour, M.R.; Raeissi, S.; Rajaei, H. Development of a detailed reaction network for industrial upgrading of heavy reformates to xylenes using differential evolution technique. *J. Taiwan Inst. Chem. Eng.* **2015**, *48*, 56–72. [[CrossRef](#)]
21. Almulla, F.; Zholobenko, V.I.; Tedstone, A.A.; Jumah, A.B.; Aldossary, M.R.; Garforth, A.A. Effect of hydrogenative regeneration on the activity of beta and Pt-beta zeolites during the transalkylation of toluene with 1,2,4-trimethylbenzene. *Microporous Mesoporous. Mater.* **2020**, *293*, 109737. [[CrossRef](#)]
22. De Lasa, H.I. Riser Simulator for Catalytic Cracking Studies. U.S. Patent No. 5,102,628, 7 April 1992.
23. De Lasa, H.I. The CREC Fluidized Riser Simulator a Unique Tool for Catalytic Process Development. *Catalysts* **2022**, *12*, 888. [[CrossRef](#)]

Disclaimer/Publisher's Note: The statements, opinions and data contained in all publications are solely those of the individual author(s) and contributor(s) and not of MDPI and/or the editor(s). MDPI and/or the editor(s) disclaim responsibility for any injury to people or property resulting from any ideas, methods, instructions or products referred to in the content.